

Fusion barrier distributions in ${}^{6,7}\text{Li} + {}^{209}\text{Bi}$ reactions from quasi-elastic and fusion excitation function measurements

D. Patel* and S. Mukherjee†

Physics Department, Faculty of Science, M. S. University of Baroda, Vadodra-390002, India

B. K. Nayak, S. V. Suryanarayana, D. C. Biswas, E. T. Mirgule, Y. K. Gupta, L. S. Danu, B. V. John, and A. Saxena

Nuclear Physics Division, Bhabha Atomic Research Centre, Mumbai-400085, India

(Received 31 March 2014; published 30 June 2014)

Fusion barrier distributions have been obtained from the measurement of the quasi-elastic scattering excitation functions at a backward angle in the reactions of ${}^{6,7}\text{Li}$ with ${}^{209}\text{Bi}$. Comparisons have been carried out among barrier distributions, obtained from quasi-elastic scattering by considering elastic + inelastic and elastic + inelastic + [breakup(BU) and/or transfer] and also from fusion excitation function measurements. It has been observed that representations of barrier distributions obtained from elastic + inelastic + [breakup(BU) and/or transfer] and from fusion excitation functions are in good agreement showing the importance of the inclusion breakup channels for the correct fusion barrier representations in the ${}^{6,7}\text{Li} + {}^{209}\text{Bi}$ reactions. The observed discrepancy in the resultant barrier distributions with and without including breakup and/or transfer has been interpreted in terms of the capture barrier distribution. The results obtained from the continuum discretized coupled channels calculations also follow the fusion barrier distributions which have been obtained from the fusion excitation functions measurements. It has been observed that the inclusion of direct breakup α with the elastic and inelastic channels in quasi-elastic scattering play an important role in explaining consistently the fusion barrier distributions for both the ${}^{6,7}\text{Li} + {}^{209}\text{Bi}$ systems.

DOI: [10.1103/PhysRevC.89.064614](https://doi.org/10.1103/PhysRevC.89.064614)

PACS number(s): 25.70.Bc, 25.70.Mn, 24.10.Eq

I. INTRODUCTION

In recent years, the investigation of fusion reactions involving either unstable nuclei, far from the valley of stability, or weakly bound stable nuclei, such as ${}^{6,7}\text{Li}$ and ${}^9\text{Be}$, has been of great relevance for the synthesis of superheavy elements and for the study of astrophysical processes [1]. The ${}^{6,7}\text{Li}$ and ${}^9\text{Be}$ nuclei display very low nucleon (cluster) breakup energies ranging from 1.47 to 2.47 MeV. The fusion cross sections are very sensitive to the structure of interacting (projectile/target) nuclei as well as impact from the coupling of other reaction channels such as breakup and nucleon transfer. In reactions involving weakly bound nuclei having cluster structure, breakup into $\alpha + x$ may occur in single step or it may take place after a nucleon transfer [2,3].

The coupling of different reaction channels produce different Coulomb barriers showing the effects on the fusion process by the enhancement or suppression of fusion cross sections at around the Coulomb barrier energies. There are two complementary methods for fusion barrier distribution determination such as either by precise fusion excitation function measurement or by quasi-elastic scattering excitation function at backward angles [4]. The complementarity of fusion barrier distributions obtained from quasi-elastic scattering and fusion is due to the fact that the ratio of $d\sigma^{\text{qel}}/d\sigma^{\text{R}}(E)$ at 180° , is the reflection coefficient R_\circ for $l = 0$ and the barrier penetration probability, T_\circ , related to fusion is unitary, that is $R^{\text{qel}}(E) + T^{\text{fus}}(E) = 1$. If new reaction channels other

than quasi-elastic scattering and fusion are present, the $T_\circ = 1 - R_\circ$, no longer represents fusion barrier penetration probability rather it gives the capture probability. In a recent work [5], it has been suggested that the barrier distributions derived from quasi-elastic scattering at backward angles of very heavy target-projectile systems leads to information about the total reaction threshold distribution, instead of the usually accepted information about the fusion barrier because of appearance of deep inelastic scattering besides quasi-elastic scattering and fusion in these systems. A similar situation can also arise in the case of reactions with loosely bound nuclei, where the break-up channel is dominant. Therefore, while dealing with weakly bound nuclei, it is required to include the direct breakup channels and breakup channels triggered by transfer reactions to the quasi-elastic excitation functions for the correct representation of fusion barrier distribution. Recently, it has been observed that in the reaction of ${}^{6,7}\text{Li}$ with ${}^{207,208}\text{Pb}$, and ${}^{209}\text{Bi}$, the breakup is predominantly triggered by transfer at below the Coulomb barrier energies [2]. Earlier, in the reaction of ${}^6\text{Li}$ with ${}^{208}\text{Pb}$, exclusive breakup measurements have been done at several energies at around the Coulomb barrier energies, and $\alpha + d$ exclusive cross sections have been reproduced by the continuum discretized coupled channels (CDCC) formalism. Large differences between inclusive and exclusive cross sections have been understood due to the stripping breakup (that is breakup followed by transfer) [6]. Diaz-Torres *et al.* [7] have obtained total (complete + incomplete) fusion excitation functions in the reaction of ${}^{6,7}\text{Li}$ with ${}^{59}\text{Co}$ and ${}^{209}\text{Bi}$ targets at Coulomb barrier energies by employing the CDCC formalism. It has been shown that breakup effects are important in enhancing the fusion cross sections at around the barrier energies as compared to the

*Corresponding author: dipika.physics@gmail.com†smukherjee_msufpy@yahoo.co.in

well-above barrier energy regime. Therefore, it would be of great interest to compare the experimental fusion barrier distributions derived from the inclusion of different channels such as breakup and transfer in a quasi-elastic excitation function. There have been few measurements on a quasi-elastic barrier distribution involving weakly bound nuclei such as ${}^6,7\text{Li}$, ${}^9\text{Be}$ [8–12]. It may be noted that the barrier distributions derived from quasi-elastic scattering involving weakly bound projectiles, without including all direct reaction parts, actually show capture barrier distribution and not actual fusion barrier distribution [5, 13].

A systematic study of fusion barrier distributions obtained by the fusion excitation function and quasi-elastic scattering along with the inclusion of breakup and/or transfer channel for both the ${}^6,7\text{Li}$ projectiles will be of interest as α yields have been observed to be produced via projectile breakup and/or transfer. The fusion barrier distributions from fusion excitation function for ${}^6,7\text{Li} + {}^{209}\text{Bi}$ systems are available in the literature [14]. In the present work, we have carried out barrier distributions for the similar systems by quasi-elastic scattering at $\theta_{\text{lab}} = 140^\circ$. The fusion barrier distributions obtained from the quasi-elastic scattering excitation functions have been compared with the fusion barrier distributions which are extracted from the experimentally measured fusion cross sections. The CDCC calculations using the FRESKO code [15] also have been carried out to interpret experimentally observed quasi-elastic scattering excitation functions and corresponding fusion barrier distributions for ${}^6,7\text{Li} + {}^{209}\text{Bi}$ systems.

II. EXPERIMENTAL DETAILS

The experiments have been performed using ${}^6,7\text{Li}^{(3+)}$ beams at the 14UD BARC-TIFR Pelletron facility in Mumbai, India. A self-supported ${}^{209}\text{Bi}$ target of thickness $\sim 1.2 \text{ mg/cm}^2$ was used. The experimental measurements have been done at 140° employing a detector telescope with the thickness of $\Delta E = 15 \mu\text{m}$ and $E = 1.5 \text{ mm}$. The spectra were recorded in the bombarding energy range from 22.0 to 39.0 MeV in steps of 1.0 MeV. Two monitor detectors were placed at $\pm 18^\circ$ for normalization and beam monitoring. The bombarding energies have been corrected for the energy loss in half the target thicknesses, ranging from 0.12 to 0.18 MeV for ${}^6\text{Li}$ and 0.14 to 0.2 MeV for the ${}^7\text{Li}$ projectile. The results of quasi-elastic at 140° have been converted to that of 180° by introducing an effective energy, into the quasi-elastic cross sections that is, $E_{\text{eff}} = 2E_{\text{c.m.}}/[1 + \text{cosec}(\theta_{\text{c.m.}}/2)]$. This corrects for centrifugal effects by making $\sigma_{qe}(E_{\text{eff}}) \approx \sigma_{qe}(E_{\text{c.m.}}, 140^\circ)$ [16]. Figure 1 shows a typical two-dimensional spectrum obtained at $E_{\text{lab}} = 34 \text{ MeV}$ and $\theta_{\text{lab}} = 140^\circ$ for the ${}^7\text{Li} + {}^{209}\text{Bi}$ system.

III. ANALYSIS AND DISCUSSION

In the present work, quasi-elastic scattering excitation function measurements have been obtained at a backward angle (140°) in the reactions of ${}^6,7\text{Li}$ with ${}^{209}\text{Bi}$, following the procedure described in Ref. [16]. Fusion barrier distributions have been obtained by including various channels in the

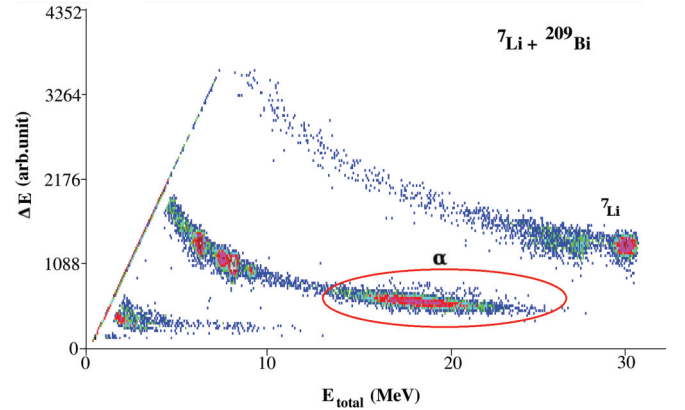


FIG. 1. (Color online) A typical two-dimensional spectrum of ΔE versus E_{tot} for ${}^7\text{Li} + {}^{209}\text{Bi}$ at $E_{\text{lab}} = 34 \text{ MeV}$ and $\theta_{\text{lab}} = 140^\circ$.

quasi-elastic scattering such as elastic, inelastic, and [breakup (BU) and/or transfer]. In a typical two-dimensional plot a distinct blob of α -particle yields peaking at $4/7$ of the laboratory energy for the reaction of ${}^7\text{Li}$ with ${}^{209}\text{Bi}$, can be clearly seen in Fig. 1. The widths of the corresponding α -particle yields at different projectile energies have been calculated using the kinematics relation for both the ${}^6,7\text{Li} + {}^{209}\text{Bi}$ systems as given in Ref. [6]. For the ${}^6\text{Li} + {}^{209}\text{Bi}$ reaction around $\sim 8\text{--}10 \text{ MeV}$ and for the ${}^7\text{Li} + {}^{209}\text{Bi}$ reaction around $\sim 13\text{--}17 \text{ MeV}$ widths of broad α -particle blobs were considered to extract the contributed α yields. In the reactions of ${}^6,7\text{Li}$ with ${}^{209}\text{Bi}$ the probability of α particles coming from the direct reactions can have different origins, mainly, direct breakup ($\alpha + d$ or $\alpha + t$) of projectiles (${}^6,7\text{Li}$) or breakup of a projectile followed by $1p$ pickup, $1n, 2n$ -stripping in the case of the ${}^7\text{Li}$ projectile. Similarly, in the reaction of ${}^6\text{Li} + {}^{209}\text{Bi}$ the BU of the projectile may occur via direct breakup, $1p, 1n$ pickup, $1n$ -stripping [2]. The α -particle yield may also have contributions from d/t transfer or capture. In the case of capture, this may lead to incomplete fusion (ICF) that may reach saturation as energy increases [17–19]. In the present analysis, in order to understand the projectile breakup effects (via breakup and/or transfer) on fusion barrier distributions, these α -particle yields have been taken as part of quasi-elastic scattering for both the ${}^6,7\text{Li}$ with ${}^{209}\text{Bi}$ reactions. The impurities from ${}^{16}\text{O}$ and ${}^{12}\text{C}$ in the observed α -particle energy peaks of our considerations are also checked from the kinematics. From the statistical model calculations it has been observed that the α particles coming from the evaporation were lower in energies. It has been observed that the breakup α peaks from the contamination of ${}^{16}\text{O}$ and ${}^{12}\text{C}$ fall below 9.0 MeV, while for the present reactions of ${}^6,7\text{Li}$ with a ${}^{209}\text{Bi}$ target peak at 20.38 and 17.18 MeV, respectively. Which confirms that contributed α particles are purely produced from the reactions of ${}^6,7\text{Li}$ with ${}^{209}\text{Bi}$.

The measured quasi-elastic excitation functions for both the ${}^6,7\text{Li} + {}^{209}\text{Bi}$ reactions have been shown in Figs. 2 and 3. The filled black points and red crosses indicate the excitation functions for elastic + inelastic and elastic + inelastic + BU and/or transfer. The CDCC calculations using the FRESKO code [15] have also been carried out to describe the quasi-elastic

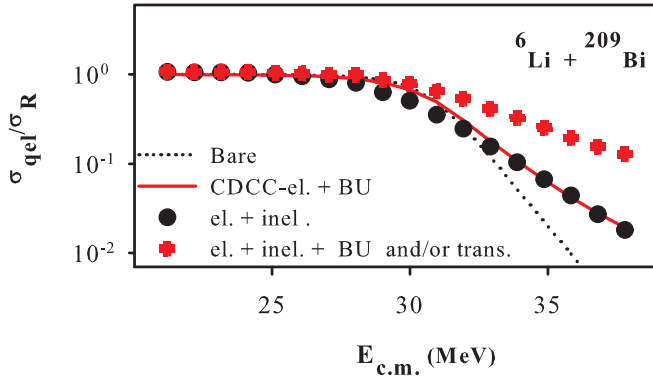


FIG. 2. (Color online) Quasi-elastic excitation function at 140° for the ${}^6\text{Li} + {}^{209}\text{Bi}$ system. The filled circles (black) show the data points with elastic + inelastic and crosses (red) show the data points with elastic + inelastic + BU and/or transfer. The dotted line indicates the results of coupled channels calculations using a bare potential. The continuous line shows the results from the CDCC calculation which includes elastic + direct breakup (BU).

scattering excitation functions and the corresponding fusion barrier distributions.

In the CDCC calculations, the projectiles ${}^6,7\text{Li}$ have been considered as $\alpha + d/t$ clusters, respectively. The continuum parts have been discretized in small momentum bins for nonresonant parts and further fine binnings have been carried out in resonant parts for both the ${}^6,7\text{Li}$ excitations. The maximum excitation energy has been taken up to ~ 9 MeV and reduced to a lower excitation for below and at the Coulomb barrier energies in the reactions of ${}^6,7\text{Li} + {}^{209}\text{Bi}$. In the case of CDCC involving the ${}^7\text{Li}$ projectile, the set of real parts of Woods-Saxon potentials for $\alpha + {}^{209}\text{Bi}$ and for $t + {}^{209}\text{Bi}$ were $V_o = 87.93$ MeV, $r_o = 1.361$ fm, $a_o = 0.578$ fm and $V_o = 130.96$ MeV, $r_o = 1.2$ fm, $a_o = 0.72$ fm, respectively. In the CDCC calculation with a ${}^6\text{Li}$ projectile, the potentials

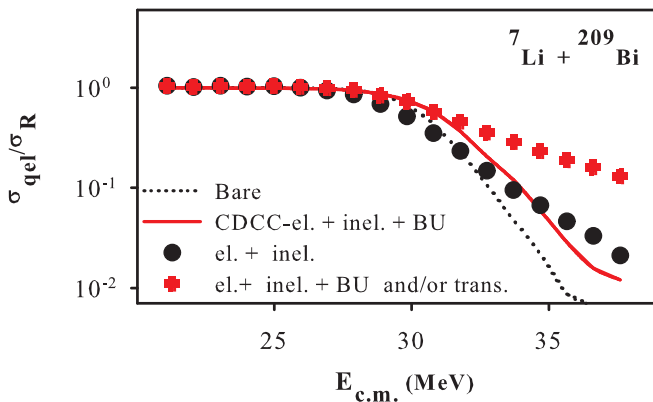


FIG. 3. (Color online) Quasi-elastic excitation function at 140° for the ${}^7\text{Li} + {}^{209}\text{Bi}$ system. The filled circles (black) show the data points with elastic + inelastic and crosses (red) show the data points with elastic + inelastic + BU and/or transfer. The dotted line indicates the results of Coupled Channels calculations using bare potential. The continuous line shows the results from CDCC calculation which includes elastic + ${}^7\text{Li}$ -inelastic + direct breakup (BU).

TABLE I. Total reaction ($\sigma_{\text{react.}}^{\text{tot}}$), integrated breakup ($\sigma_{\text{BU}}^{\text{inte.}}$), and breakup cross sections at 140° ($\sigma_{\text{BU}}^{140^\circ}$) from the CDCC calculation and α cross sections at 140° ($\sigma_\alpha^{140^\circ}$) from the experiment for the ${}^6\text{Li} + {}^{209}\text{Bi}$ system.

$E_{\text{c.m.}}$ (MeV)	$\sigma_{\text{react.}}^{\text{tot}}$ (mb) (CDCC)	$\sigma_{\text{BU}}^{\text{inte.}}$ (mb) (CDCC)	$\sigma_{\text{BU}}^{140^\circ}$ (mb/sr) (CDCC)	$\sigma_\alpha^{140^\circ}$ (mb/sr) (Expt.)
21.21	13	7	1.3	1 ± 0.0
22.19	18	12	1.3	2 ± 0.0
23.16	24	16	1.5	2 ± 0.0
24.14	30	20	1.6	4 ± 0.0
25.12	38	24	1.9	7 ± 0.0
26.09	48	30	2.4	10 ± 0.0
27.07	62	36	2.9	16 ± 0.0
28.04	81	42	2.4	23 ± 0.0
29.02	114	47	2.4	28 ± 0.01
29.99	165	54	3.0	32 ± 0.01
30.97	238	63	3.3	31 ± 0.02
31.94	328	71	2.9	28 ± 0.02
32.92	425	79	2.4	24 ± 0.04
33.89	520	86	2.2	20 ± 0.06
34.87	613	93	1.9	16 ± 0.11
35.84	701	100	1.6	12 ± 0.22
36.81	787	107	1.3	9 ± 0.43
37.79	868	113	0.9	8 ± 0.61

for $\alpha/d + {}^{209}\text{Bi}$ were also of Woods-Saxon form with $V_o = 60.42$ MeV, $r_o = 1.361$ fm, $a_o = 0.578$ fm and $V_o = 42.20$ MeV, $r_o = 1.150$ fm, $a_o = 0.972$ fm, respectively. The imaginary parts have been taken as an internal Woods-Saxon potential with $W_o = 30.0$ MeV, $r_o = 1.04$ fm, and $a_o = 0.2$ fm, to exclude the double counting of the effect of inelastic excitation on the elastic channel. The potentials for the ground state of ${}^6\text{Li}$ and bound state at $(1/2^+, 0.478$ MeV) of ${}^7\text{Li}$ and resonant states of ${}^6,7\text{Li}$ projectiles have been taken from Ref. [7]. The scattering wave functions in the solution of coupled-channels calculations were integrated up to 200 fm in steps of 0.05 fm and the relative angular momentum is taken up to $150\hbar$. The present calculations have been carried out without considering target inelastic states as the effects of target inelastic states are found to be insignificant [20]. The effects of transfer couplings have not been included in the present calculation as it is difficult to couple transfer channels along with the CDCC calculation because of the large spin of ${}^{209}\text{Bi}$. However, the effects from the $1n$ -stripping channel on the quasi-elastic excitation function have been investigated by coupled reaction channels calculations for the ${}^6\text{Li} + {}^{209}\text{Bi}$ reaction. This has shown that the effect from the $1n$ -stripping channel on the quasi-elastic excitation function is insignificant [21]. Also, for the reaction of ${}^7\text{Li}$ with ${}^{144}\text{Sm}$, no effect from the $1n$ -stripping channel was observed on the quasi-elastic scattering excitation function [12]. In Tables I and II, total reaction cross sections and BU cross sections have been given along with the experimental $\sigma_\alpha^{140^\circ}$, for the ${}^6,7\text{Li} + {}^{209}\text{Bi}$ systems. It can be observed that BU cross sections are dominant for ${}^6\text{Li}$ as compared to that of ${}^7\text{Li}$. In Ref. [22], for the ${}^6,7\text{Li} + {}^{59}\text{Co}$ systems, elastic scattering, excitation functions for sub- and near-barrier fusion cross sections, and breakup yields have been analyzed

TABLE II. Total reaction ($\sigma_{\text{react.}}^{\text{tot.}}$), integrated breakup ($\sigma_{\text{BU}}^{\text{inte.}}$), and breakup cross sections at 140° ($\sigma_{\text{BU}}^{140^\circ}$) from the CDCC calculation and α cross sections at 140° ($\sigma_\alpha^{140^\circ}$) from the experiment for the ${}^7\text{Li} + {}^{209}\text{Bi}$ system.

$E_{\text{c.m.}}$ (MeV)	$\sigma_{\text{react.}}^{\text{tot.}}$ (mb) (CDCC)	$\sigma_{\text{BU}}^{\text{inte.}}$ (mb) (CDCC)	$\sigma_{\text{BU}}^{140^\circ}$ (mb/sr) (CDCC)	$\sigma_\alpha^{140^\circ}$ (mb/sr) (Expt.)
21.10	50	1	0.1	—
22.07	54	1	0.1	—
23.04	58	2	0.2	—
24.01	62	2	0.2	1 ± 0.0
24.99	67	3	0.3	1 ± 0.0
25.96	72	4	0.4	4 ± 0.0
26.93	78	7	0.9	7 ± 0.0
27.90	94	10	1.2	12 ± 0.0
28.87	120	14	1.4	18 ± 0.0
29.84	170	20	1.3	24 ± 0.01
30.81	243	25	1.9	23 ± 0.01
31.78	336	30	1.2	23 ± 0.03
32.75	434	32	0.8	20 ± 0.05
33.72	533	37	0.8	17 ± 0.10
34.69	630	40	0.5	14 ± 0.18
35.66	721	46	0.5	11 ± 0.31
36.63	810	50	0.5	10 ± 0.47
37.60	892	58	0.7	8 ± 1.91

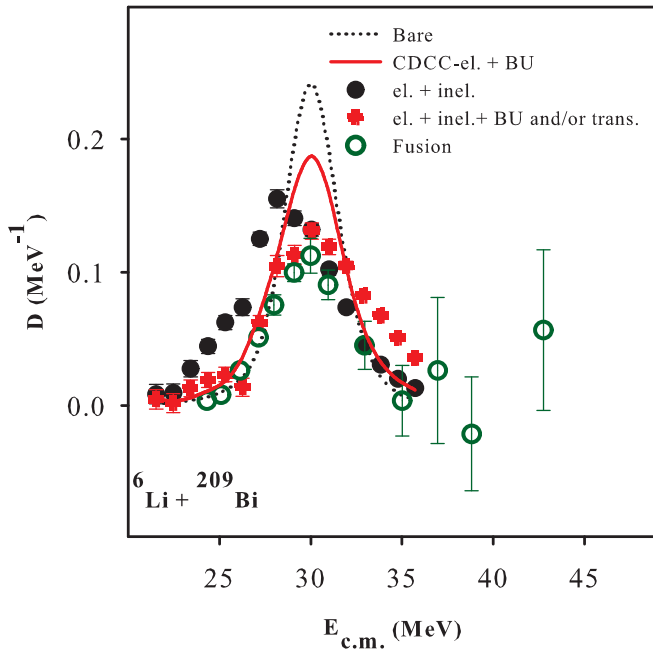


FIG. 4. (Color online) Fusion barrier distributions for the ${}^6\text{Li} + {}^{209}\text{Bi}$ system at 140° . The filled circles (black) show the data points with elastic + inelastic and crosses (red) show the data points with elastic + inelastic + BU and/or transfer. The data points shown by unfilled circles are taken from Ref. [14]. The dotted line indicates the results of coupled channels calculations using a bare potential. The continuous line shows the results from CDCC calculation which includes elastic + direct breakup (BU).

in terms of extended CDCC calculations, that also show a significant role of breakup for the ${}^6\text{Li}$ rather than ${}^7\text{Li}$ projectile.

The dotted line indicates the results of coupled channels calculations using a bare potential as shown in Figs. 2 to 5. In Figs. 2 and 4 the continuous line shows the results of CDCC calculations for ${}^6\text{Li}$ with elastic + direct breakup of ${}^6\text{Li}$. In Figs. 3 and 5 the continuous line shows the results of CDCC calculations for ${}^7\text{Li}$ with elastic + ${}^7\text{Li}$ -inelastic + direct breakup of ${}^7\text{Li}$. The fusion barrier distributions from fusion excitation functions have been shown as open circles in Figs. 4 and 5. These have been compared with the present quasi-elastic barrier distributions which have been obtained with the addition of BU and/or transfer to the elastic and inelastic channel. It has been seen that the inclusion of BU and/or transfer to the elastic and inelastic channels gives a reasonable agreement with the fusion barrier distributions which have been obtained from the fusion excitation functions as shown in Figs. 4 and 5. It reveals that to extract the correct fusion barrier distribution, the inclusion of projectile breakup and/or transfer reaction parts are of paramount importance in the reaction studies involving weakly bound nuclei.

Moreover, the transmission or capture probability (T_c) has been extracted for the present quasi-elastic excitation function using the relation $R^{\text{qel}}(E) + T^{\text{fus}}(E) = 1$ and from

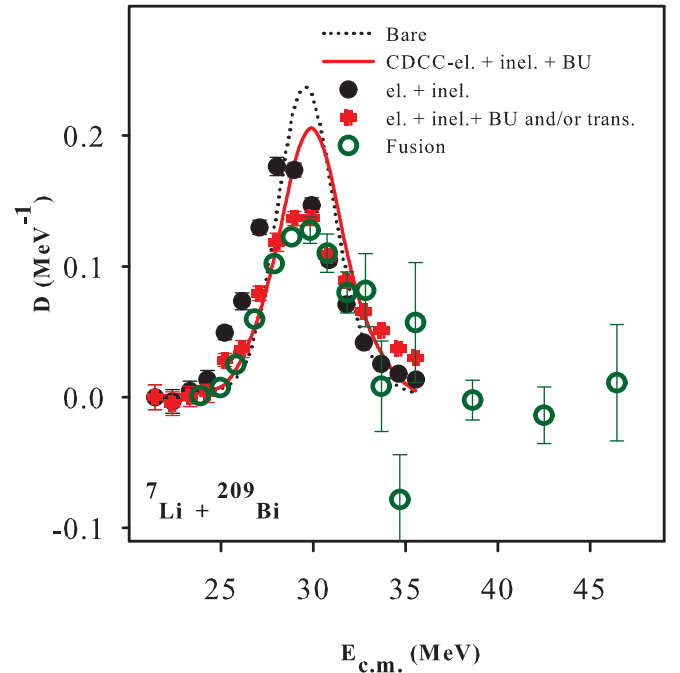


FIG. 5. (Color online) Fusion barrier distributions for the ${}^7\text{Li} + {}^{209}\text{Bi}$ system at 140° . The filled circles (black) show the data points with elastic + inelastic and crosses (red) show the data points with elastic + inelastic + BU and/or transfer. The data points shown by unfilled circles are taken from Ref. [14]. The dotted line indicates the results of coupled channels calculations using a bare potential. The continuous line shows the results from the CDCC calculation which includes elastic + ${}^7\text{Li}$ -inelastic + direct breakup (BU).

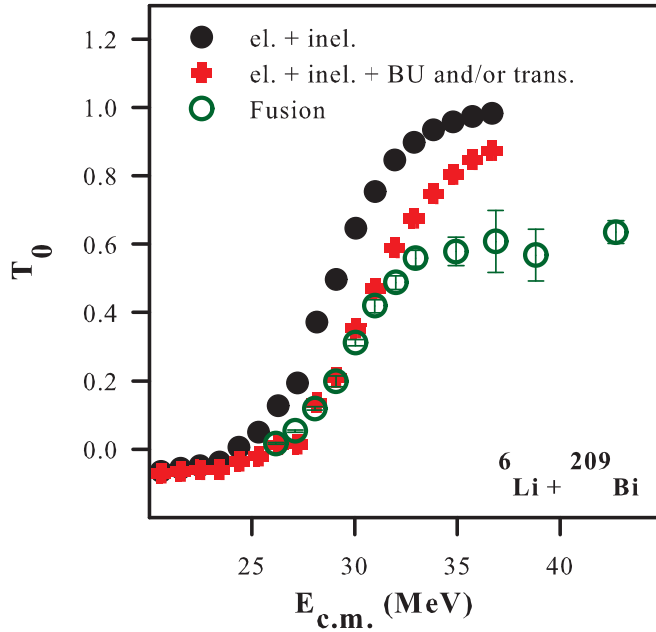


FIG. 6. (Color online) Transmission or capture probability (T_0) as a function of $E_{c.m.}$ in the reaction of ${}^6\text{Li}$ with ${}^{209}\text{Bi}$. The filled circles (black) show the data points with elastic + inelastic and crosses (red) show the data points with elastic + inelastic + BU and/or transfer. The data points shown by unfilled circles are taken from Ref. [14].

the fusion excitation function by the relation $\frac{1}{\pi R_b^2} \frac{d(\sigma \cdot E)}{dE}$ [14]. Transmission or capture probabilities (T_0) for both the reactions of ${}^{6,7}\text{Li}$ with ${}^{209}\text{Bi}$, have been plotted as a function of $E_{c.m.}$ as shown in Figs. 6 and 7. It has been observed that the transmission or capture probabilities which are derived from the fusion excitation functions indicate good agreement with the one from the present quasi-elastic scattering data except at well above the Coulomb barrier energies for ${}^{6,7}\text{Li} + {}^{209}\text{Bi}$ reactions. There is an overall shift between the (T_0) curves obtained from quasi-elastic scattering corresponding to elastic + inelastic channels and elastic + inelastic + BU and/or transfer channels. This shift is more for the ${}^6\text{Li} + {}^{209}\text{Bi}$ reaction compared to the ${}^7\text{Li} + {}^{209}\text{Bi}$ reaction which is co-related with the projectile breakup threshold energy. Therefore, this suggests that due to the lower breakup threshold the energy shift is more.

IV. SUMMARY AND CONCLUSION

The fusion barrier distributions have been obtained from the quasi-elastic excitation function measurements at $\theta_{lab} = 140^\circ$ for ${}^{6,7}\text{Li} + {}^{209}\text{Bi}$ systems. The fusion barrier distributions derived from experimental quasi-elastic data have been compared with the fusion barrier distributions obtained from the fusion excitation function measurements [14] for ${}^{6,7}\text{Li} + {}^{209}\text{Bi}$ systems. The fusion barrier distributions obtained from quasi-elastic and fusion excitation function measurements are observed to be consistent only when BU and/or transfer channels are added to the quasi-elastic events. The

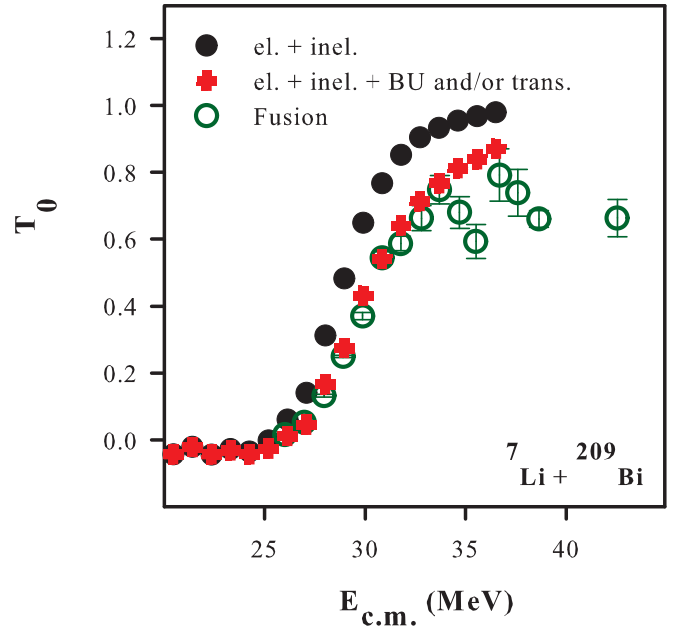


FIG. 7. (Color online) Transmission or capture probability (T_0) as a function of $E_{c.m.}$ in the reaction of ${}^7\text{Li}$ with ${}^{209}\text{Bi}$. The filled circles (black) show the data points with elastic + inelastic and crosses (red) show the data points with elastic + inelastic + BU and/or transfer. The data points shown by unfilled circles are taken from Ref. [14].

transmission or capture probabilities (T_0) obtained from the present quasi-elastic excitation functions have been compared with those obtained from the fusion excitation functions which indicates reasonable agreement at near barrier energies for reactions of ${}^{6,7}\text{Li}$ with ${}^{209}\text{Bi}$.

The CDCC calculations using the FRESKO code [15] also have been carried out to interpret experimentally obtained quasi-elastic scattering excitation functions and the corresponding barrier distributions. While deriving fusion barrier distributions from the CDCC calculations, direct breakup of ${}^6,7\text{Li}$ projectiles has also been incorporated to the ${}^6\text{Li}$ -elastic and ${}^7\text{Li}$ -elastic plus inelastic channels, respectively. The fusion barrier distributions which have been obtained from the CDCC calculation and experimental data shows similar peak positions. Though, from the present calculations the barrier heights are observed to be different from the experimental one which may be due to the contributions from other reaction channels, such as nucleon transfer, sequential breakup [23] which have not been included in the present CDCC calculations.

ACKNOWLEDGMENTS

The authors thank Prof. J. Lubian for his help in some of the calculations. D.P., acknowledges support by HRDG-CSIR (Ack. No. 162033/2K12/1), India.

- [1] B. B. Back, H. Esbensen, C. L. Jiang, and K. E. Rehm, *Rev. Mod. Phys.* **86**, 317 (2014).
- [2] D. H. Luong, M. Dasgupta, D. J. Hinde, R. du Rietz, R. Rafiei, C. J. Lin, M. Evers, and A. Diaz-Torres, *Phys. Rev. C* **88**, 034609 (2013).
- [3] D. Patel, S. Santra, S. Mukherjee, B. K. Nayak, P. K. Rath, V. V. Parkar, and R. K. Choudhury, *Pramana J. Phys.* **81**, 587 (2013).
- [4] S. Mitsuoka, H. Ikezoe, K. Nishio, K. Tsuruta, S. C. Jeong, and Y. Watanabe, *Phys. Rev. Lett.* **99**, 182701 (2007).
- [5] S. S. Ntshangase, N. Rowley, R. A. Bark, S. V. Fritsch, J. J. Lawrie, E. A. Lawrie, R. Lindsay, M. Lipoglavsek, S. M. Maliage, L. J. Mudau *et al.*, *Phys. Lett. B* **651**, 27 (2007).
- [6] C. Signorini, A. Edifizi, M. Mazzocco, M. Lunardon, D. Fabris, A. Vitturi, P. Scopel, F. Soramel, L. Stroe, G. Prete *et al.*, *Phys. Rev. C* **67**, 044607 (2003).
- [7] A. Diaz-Torres, I. J. Thompson, and C. Beck, *Phys. Rev. C* **68**, 044607 (2003).
- [8] S. Mukherjee, B. K. Nayak, D. S. Monteiro, J. Lubian, P. R. S. Gomes, S. Appannababu, and R. K. Choudhury, *Phys. Rev. C* **80**, 014607 (2009).
- [9] D. Patel, B. K. Nayak, S. Mukherjee, D. C. Biswas, E. T. Mirgule, B. V. John, Y. K. Gupta, S. Mukhopadhyay, G. Prajapati, L. S. Danu *et al.*, *AIP Conf. Proc.* **1524**, 171 (2013).
- [10] M. Zadro, P. Figuera, A. Di Pietro, M. Fisichella, M. Lattuada, T. Lönnroth, M. Milin, V. Ostashko, M. G. Pellegriti, V. Scuderi *et al.*, *Phys. Rev. C* **87**, 054606 (2013).
- [11] H. M. Jia, C. J. Lin, H. Q. Zhang, Z. H. Liu, N. Yu, F. Yang, F. Jia, X. X. Xu, Z. D. Wu, S. T. Zhang, and C. L. Bai, *Phys. Rev. C* **82**, 027602 (2010).
- [12] D. R. Otomar, J. Lubian, P. R. S. Gomes, D. S. Monteiro, O. A. Capurro, A. Arazi, J. O. Fernandez Niello, J. M. Figueira, G. V. Mart, D. Martinez Heimann *et al.*, *Phys. Rev. C* **80**, 034614 (2009).
- [13] V. I. Zagrebaev, *Phys. Rev. C* **78**, 047602 (2008).
- [14] M. Dasgupta, P. R. S. Gomes, D. J. Hinde, S. B. Moraes, R. M. Anjos, A. C. Berriman, R. D. Butt, N. Carlin, J. Lubian, C. R. Morton *et al.*, *Phys. Rev. C* **70**, 024606 (2004).
- [15] I. J. Thompson, *Comput. Phys. Rep.* **7**, 167 (1988).
- [16] H. Timmers, J. R. Leigh, M. Dasgupta, D. J. Hinde, R. C. Lemmon, J. C. Mein, C. R. Morton, J. O. Newton, and N. Rowley, *Nucl. Phys. A* **584**, 190 (1995).
- [17] A. Diaz-Torres, *J. Phys. G: Nucl. Part. Phys.* **37**, 075109 (2010).
- [18] F. A. Souza, N. Carlin, C. Beck, N. Keeley, A. Diaz-Torres, R. Liguori Neto, C. Siqueira-Mello, M. M. de Moura, M. G. Munhoz, R. A. N. Oliveira *et al.*, *Nucl. Phys. A* **834**, 420c (2010).
- [19] C. Beck, *Nucl. Phys. A* **787**, 251 (2007).
- [20] S. Santra, S. Kailas, K. Ramachandran, V. V. Parkar, V. Jha, B. J. Roy, and P. Shukla, *Phys. Rev. C* **83**, 034616 (2011).
- [21] D. Patel, S. V. Suryanarayana, S. Mukherjee, B. K. Nayak, E. T. Mirgule, D. C. Biswas, A. Saxena, and J. Lubian (private communication).
- [22] C. Beck, N. Keeley, and A. Diaz-Torres, *Phys. Rev. C* **75**, 054605 (2007).
- [23] D. R. Otomar, J. Lubian, P. R. S. Gomes, and T. Correa, *J. Phys. G: Nucl. Part. Phys.* **40**, 125105 (2013).